Influence of sizing strategy and control rules on the energy saving potential of heat pump hybrid systems in a residential building

Published Version:
Dongellini Matteo, Naldi Claudia, Morini Gian Luca (2021). Influence of sizing strategy and control rules on the energy saving potential of heat pump hybrid systems in a residential building. ENERGY CONVERSION AND MANAGEMENT, 235, 1-12 [10.1016/j.enconman.2021.114022].

Availability:
This version is available at: https://hdl.handle.net/11585/843167 since: 2024-05-13

Published:
DOI: http://doi.org/10.1016/j.enconman.2021.114022

Matteo Dongellini, Claudia Naldi, Gian Luca Morini

Influence of sizing strategy and control rules on the energy saving potential of heat pump hybrid systems in a residential building

In: Energy Conversion and Management, Volume 235, 2021, 114022

Influence of sizing strategy and control rules on the energy saving potential of heat pump hybrid systems in a residential building

Matteo Dongellini[a,*], Claudia Naldi[a], Gian Luca Morini[a]

[a] *Department of Industrial Engineering*

Alma Mater Studiorum - University of Bologna

Viale Risorgimento 2, 40136, Bologna, Italy

*Corresponding author:

Tel: +39 051 2090567

Fax: +39 051 2093296

E-mail: matteo.dongellini@unibo.it

Other e-mails: claudia.naldi2@unibo.it; gianluca.morini3@unibo.it

ABSTRACT

Hybrid heat pump systems are a suitable solution to mitigate the well-known disadvantages of air-source heat pumps, such as energy losses linked to defrost cycles and a significant reduction of their heating capacity during the most severe part of the season: in hybrid systems the heat pump is sized to satisfy only a fraction of the building peak load and is coupled to a second heater (back-up device), which helps the heat pump during the coldest part of the winter. In this paper, a series of dynamic simulations has been performed to calculate the seasonal performance of hybrid systems based on an air-to-water heat pump and to assess the optimal configuration of the system. Results point out that the energy performance of these systems strongly depends on the heat pump sizing, the back-up device typology and the control algorithm used for the activation of the heat generators. It is demonstrated that the adoption of hybrid systems in which the heat pump is coupled to a gas boiler allows to obtain relevant primary energy savings. The overall seasonal efficiency can be increased up to 6% and 22%, if compared to monovalent systems respectively based on a heat pump or a gas boiler, only if the heaters are activated following an alternative operating mode, with a cut-off temperature selected between the design and the bivalent temperature. On the contrary, if the back-up device of the hybrid system is an electric resistance, the heaters have to work in parallel during the whole heating season and the only achievable advantage is that the heat pump can be slightly under-sized with respect to the nominal building load.

Keywords: hybrid heat pump system; air-to-water heat pump; gas-fired boiler; cycling losses; control strategy; system energy performance.

NOMENCLATURE

Abbreviations

AWHP	Air-to-water heat pump
B	Boiler
BES	Building energy signature
EEV	Electronic expansion valve
ER	Electric resistance
HDD	Heating degree day
HHP	Hybrid heat pump
HP	Heat pump
LHV	Lower heating value
TEV	Thermostatic expansion valve
TMY	Typical meteorological year

Symbols

COP	Coefficient of performance	
E	Energy	(kWh)
K_p	Proportional gain	
P	Power	(kW)
PEF	Primary energy factor	(kWh_p/kWh)
t	Time	(s)
T	Temperature	(°C)
T_{biv}	Bivalent temperature	(°C)
$T_{cut\text{-}off}$	Cut-off temperature	(°C)

T_{des}	Design temperature	(°C)
t_i	Integral time	(s)
$SCOP$	Seasonal coefficient of performance	
$SCOP_{net}$	Net seasonal coefficient of performance	

Greek symbols

β	Peak load ratio	
η_B	Boiler seasonal efficiency	
η_{ER}	Electric resistance seasonal efficiency	
η_g	Boiler efficiency	
η_S	Heating system seasonal efficiency	
τ	Time constant	(s)
φ	Part load factor	
Φ	Inverter frequency	(Hz)

Subscripts

bu	back-up heater
del	delay
des	design
ee	electric energy
ext	external
gas	natural gas
gen	main heat generator
h	heating

j	index for j-th heater
i	index for i-th energy vector
in	inlet
off	shut-down transient
on	start-up transient
out	outlet
p	primary
set	set-point
th	thermal
tot	total
w	water

1. INTRODUCTION

Nowadays it is well established that the building sector significantly contributes to primary energy demand and greenhouse gas (GHG) emissions of the developed countries [1]. The European Commission agreed on a series of challenging targets to be achieved before 2030 [2]-[5]: (i) 40% reduction of GHG emissions with respect to 1990 levels; (ii) at least 27% share of renewable energy sources (increased to 32% in 2018) and (iii) at least 27% energy efficiency increase with respect to the baseline scenario (upgraded to 32.5% in 2018).

Due to the dramatic crisis of the construction sector which occurred during the last years, it is common knowledge that the above-mentioned targets can only be achieved by renewing the existing building stock: for example, in Italy the annual rate of new constructions is very low and ranges within 0.1-0.2% of the actual building stock [6]. The primary energy consumption of existing buildings can be reduced with the refurbishment of the building envelope components and/or with the retrofit of the Heating, Ventilation and Air Conditioning (HVAC) system.

In this frame, electric heat pumps may represent a promising solution to achieve the environmental targets introduced by the European Union. In fact, under current electricity grid mixes, in the major part of the world regions this kind of devices are already less GHG emission intensive than traditional HVAC systems based on fossil fuels [7]-[8]. In addition, heat pumps have the potential to exploit a significant amount of renewable energy by using aerothermal, geothermal and hydrothermal energy sources during their operation [9]. Moreover, in recent years the use of heat pumps in HVAC systems has spread widely for many other reasons [10]: (i) the capability to cover with a single device both space heating and cooling, as well as domestic hot water production; (ii) the strong improvement of their energy performance and reliability; (iii) the wider diffusion of on-site renewable electric energy generators as PV systems and the evolution of electricity prices [11].

In the European market, outdoor air is the most widespread heat source for heat pumps [10]. Air-source devices have a lot of well-known benefits, such as the availability of the external source and their low investment cost (with respect to ground-source and water-source units); on the other hand, their diffusion is held back by several unfavorable characteristics which do not allow to completely exploit the energy saving potential of these devices. First, during the coldest part of the heating season, the air-source heat pump heating capacity is reduced and its Coefficient of Performance (*COP*) decreases, while the building thermal load is at its maximum value [12]. Moreover, the well-known phenomenon of the frost deposition on the outdoor heat exchanger surface during the most severe period of the heating season and the consequent energy losses linked to defrosting cycles penalize the seasonal energy performance of these devices. More in detail, the degradation effect of frosting phenomena is twofold: on the one hand, defrosting cycles lower the heat pump heating capacity and the overall energy efficiency of the system [13]; on the other hand, the unavoidable interruption of indoor heating during the cycles may adversely affect the building occupants' thermal comfort [14].

Last but not least, if the air-source heat pump is sized to cover the building peak load in correspondence of the outdoor design temperature, the unit would operate at partial load during the whole heating period, since the peak load occurs only for a limited period of the season; for this reason, the seasonal performance factor of the system could be strongly reduced due to the excessive number of on-off cycles, activated even in presence of inverter-driven compressors [15].

In order to mitigate and in some cases to avoid the highlighted drawbacks, one possible solution is the adoption of hybrid heat pump (HHP) systems: in this configuration the air-source heat pump is sized to cover only a fraction of the building peak load and a second heat generator (also called back-up heater) supports the heat pump operation when its heating capacity is insufficient. Moreover, the back-up device can also be operated in place of the heat pump whenever its operation is not ecologically or economically viable.

The adoption of HHP systems can be crucial for the energy retrofit of heating systems in existing buildings where high-temperature terminal units, such as cast-iron radiators, are present. In fact, heat pumps are generally characterized by a limited temperature range for the produced hot water, which can be only partially in agreement with the requests of high-temperature terminal units. In this case, during the most severe period of the heating season, when the required supply temperature increases, the back-up device can help the heat pump to reach the desired supply temperature. Furthermore, the back-up heater can reduce the negative effects due to defrosting by replacing the heat pump during the activation of defrost cycles. Last but not least, in existing buildings where a conventional generation system based on a gas/oil boiler is present, the boiler can be fruitfully used as back-up device with no additional investment costs.

At the moment, the market share of hybrid heat pump systems in Europe is still limited but is rapidly growing. In 2014 only about 6500 HHP systems were sold in the whole European market but in 2017 almost 6700 HHP devices were sold by considering only the Italian market, doubling the sales of HHP in Italy of 2015 [16]. Moreover, a recent study on the European market of HHPs shows that a number of sales close to 40000 HHPs units is expected in 2020 [17].

Due to the increasing interest of the market for HHP systems, a series of scientific works has been recently conducted with the aim to investigate and optimize the energy performance of different kinds of hybrid systems involving air-source heat pumps and back-up heaters.

Park et al. [18] developed a numerical model of a hybrid system consisting of an air-to-water heat pump (AWHP) and a gas-fired water heater coupled to a typical residential apartment. The energy performance and the economic feasibility of the proposed system were investigated by the authors, who concluded that the achievable energy savings are strongly influenced by the effective control strategy of the hybrid water heater. The importance of control algorithms for these systems has been also highlighted by De Coninck and Helsen [19]: they implemented a Modelica grey-box model of a HHP system composed by two AWHPs and a condensing gas boiler, comparing the efficiency of a model-predictive and a rule-based control logic. Results pointed out that the predictive controller could guarantee similar thermal comfort and energy cost savings up to 40% with respect to the standard control. Li [20] proposed an innovative economic-based control logic for a parallel loop hybrid system composed by an AWHP and a gas-fired water heater. According to this logic, the optimal working point of the system (i.e. mass flow rate and supply water set-point temperature for each device) can be evaluated and significant economic benefits up to 60% can be obtained with respect to a traditional solution. Li and Du [21] investigated the energy and economic performance of a hybrid system in which an AWHP and a gas boiler are connected in series. They compared the effectiveness of two control algorithms used for the activation of the heat generators and the optimization of their operating modes. Results pointed out that with both control strategies significant energy savings can be achieved and the best performance is obtained when both heat devices are simultaneously activated. Furthermore, other researchers have recently demonstrated that this topic is worth to be investigated: these analyses point out that the optimization of HHP systems control logic by means of cost-adaptive and demand-response algorithms is a simple and cost-effective solution to obtain with HHP systems energy and economic savings up to 22% ([22]-[26]).

Another important parameter for the optimization of the energy savings achievable with the adoption of HHP systems is the choice of the size of the heating system components (boiler, heat pump, thermal storage) and its consequences on the algorithm by means of which the control system decides to switch on or off the heaters. In the literature, few studies have already focused on this topic. For instance, Bagarella et al. [27] analyzed, by means of dynamic simulations, how the control system of the heaters of a hybrid system (i.e. heat pump and gas boiler) affects the seasonal efficiency of the system. They analyzed two different working modes for the hybrid system: i) the operating mode in which heat pump and boiler are switched on alternatively; ii) the operating mode in which heat pump and boiler work in parallel. The authors used the numerical results in order to assess the optimal values of control setting for HHP systems. The same topic was studied by Fischer et al. [28]: the optimal size of the main elements of a hybrid system (PV panels, air-source heat pump, electric boiler and thermal storage) was investigated taking into account electricity price, profile of space heating loads, domestic hot water demand and photovoltaic field size. Results showed that, in order to obtain the maximum energy performance, the profile of the heating load should be considered in detail. Similar results have been obtained by Klein et al. [29]: annual simulations of a hybrid heat pump system were performed by varying the insulation of the building envelope, the volume of the thermal storage and the heat pump size; the results of this work highlight that the influence of the thermal storage volume on the seasonal performance of the system is negligible while the maximum efficiency can be achieved with heat pumps sized to cover only a fraction of the building peak load. Furthermore, Di Perna et al. [30] compared the energy performance of monovalent and bivalent heating systems considering different kinds of heat generators (i.e. oil and gas boiler, micro CHP, heat pump) and back-up unit (i.e. electric heater and gas boiler). They found that the electrical back-up systems are not a profitable solution.

The analysis of the literature points out that only few studies on HHP systems include, at the same time, a detailed modeling of both building and heating system components (i.e. by taking into account the energy penalties due to defrosting and on-off cycles of the heat pump), the evaluation of the best system layout and the optimization of the control strategy. In this work a numerical investigation of the seasonal energy performance of a HHP system composed by an air-to-water heat pump coupled in series to a back-up device (an electric resistance or a condensing gas boiler) is presented. The analysis is focused on the optimization of the HHP system energy performance during the winter season only, that is often an important part of the annual operating time of heat pumps coupled to residential buildings in cold climates. The dynamic model of the hybrid system has been developed by means of TRNSYS 17 [31]. The main goal of this investigation is to analyze the role played by the back-up typology (electrical resistance or gas-fired boiler), by the system control logic and by the heat pump sizing with respect to the design building heating load on the seasonal performance factor of the HHP system. A series of simulations has been carried out, taking into account different configurations of the system. In these simulations, unlike in the most part of similar works appeared recently in the literature ([18]-[26], [28]), the energy losses linked to both the heat pump on-off cycling and to the defrost cycles have been considered. These energy losses can strongly influence the overall performance of a hybrid system based on an air-source heat pump during the winter season (especially in climatic regions where the ambient temperature stays between 0°C and 6°C during the winter, like in large part of Italy) and their evaluation is crucial in order to obtain a realistic evaluation of the seasonal energy performance of HHP systems [32].

2. METHODOLOGY

2.1. Layout of simulated systems

Different kinds of HHP systems and conventional heating systems based on a single generator (condensing gas boiler or air-to-water heat pump) were firstly implemented in TRNSYS in order to evaluate and compare their seasonal energy performance: in Figure 1 the layout of the simulated systems is shown. ~~It is important to stress that all the~~

~~elements reported in Figure 1 have been modelled within TRNSYS, by means of components included in the standard libraries of the software and by means of innovative dynamic models developed by the Authors and described in [33].~~

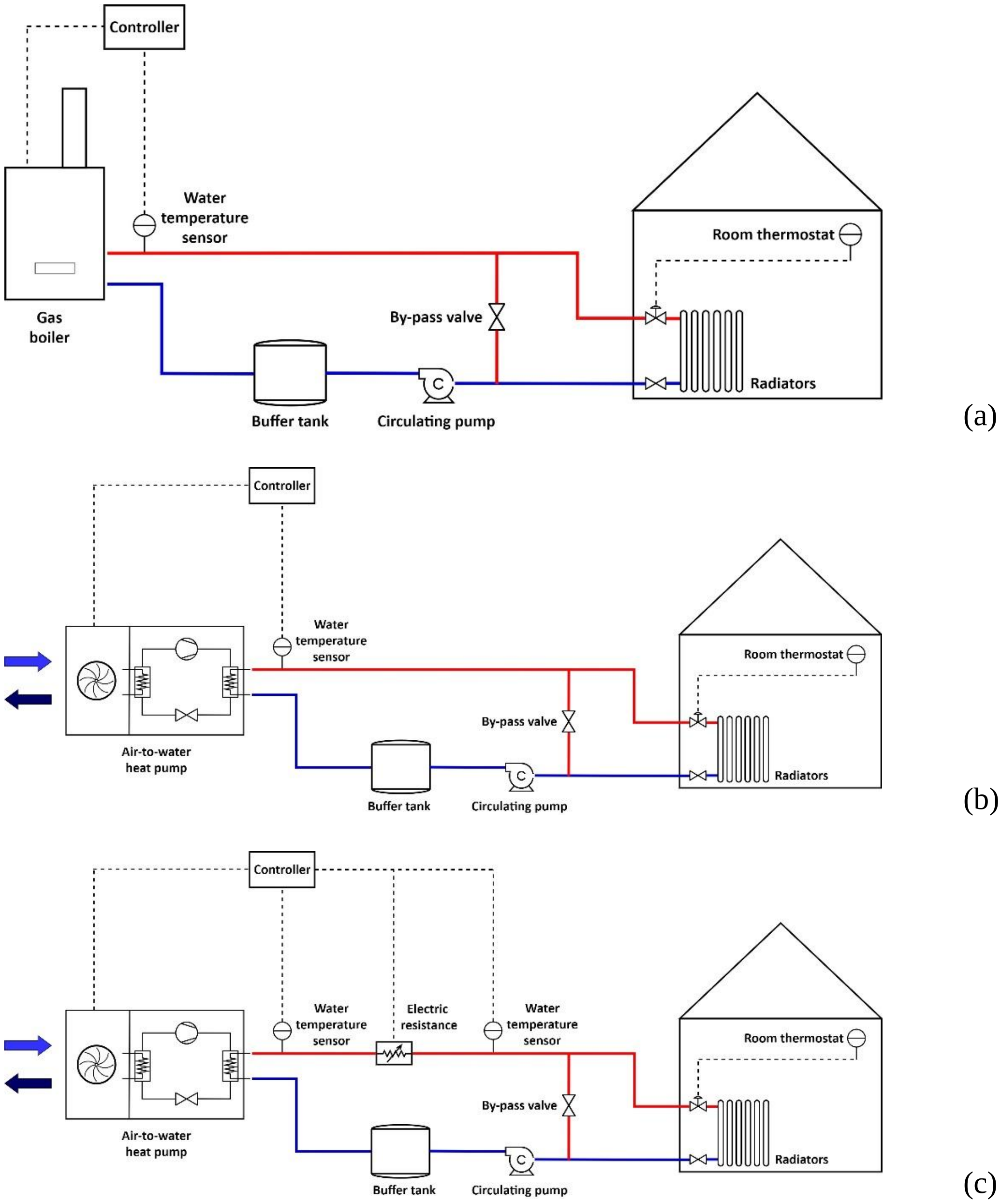

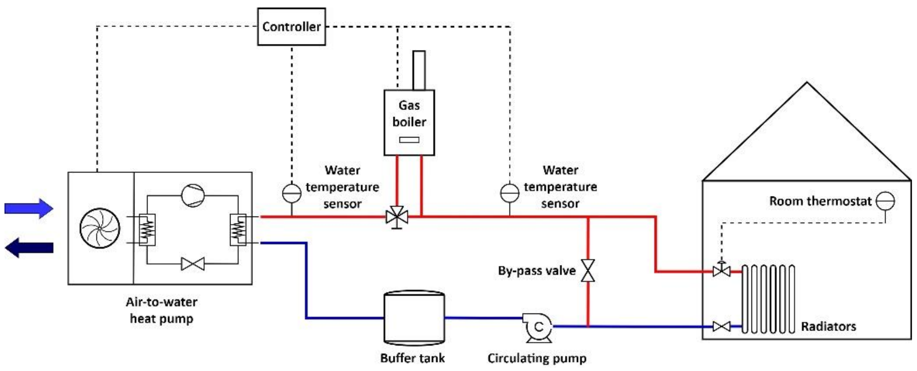

(d)

Figure 1. Layout of the simulated heating systems: (a) condensing gas boiler only, (b) air-to-water heat pump only, (c) HHP system based on air-to-water heat pump and electric resistance, (d) HHP system based on air-to-water heat pump and condensing gas boiler.

All the elements reported in Figure 1 have been modelled in TRNSYS, by using standard components included in the software libraries as well as original dynamic models developed by the Authors and described in [33]. More in detail, the basic elements of the heating systems have been modelled with standard components: Type534 is used for the buffer tank, Type114 simulates the single speed pump, while the radiators consist of a series of Types 362. The system control logics have been implemented through Type2d (on-off thermostat) and Type23 (PID controller). The performance of the condensing gas boiler has been evaluated with the boiler block (Type700) in combination with Type581, by means of which the efficiency of this device has been calculated. Electric resistances were simulated with Type6 (auxiliary heater), while specific components, as introduced by the Authors in Ref. [33], has been used to simulate the behavior of the inverter-driven air-to-water heat pumps.

First of all, the monovalent systems illustrated in Figure 1a and Figure 1b are considered as baselines for the energy performance analysis carried out in this paper. In these configurations the heating system is based on a single heat generator, a gas boiler (Figure 1a) or an air-to-water heat pump (Figure 1b). In these cases, the generator has been sized to cover the building heating peak load; in this way, the required energy demand of the building is matched during the whole winter season.

On the contrary, in HHP systems the air-to-water heat pump is coupled to a back-up device (electrical heater in Figure 1c or gas boiler in Figure 1d, respectively). In these cases, the heat pump size is reduced because a fraction of the heating load is covered by the back-up system. The heat generators of these configurations are connected in series, in order to improve the heat pump energy performance according to a lower sink temperature.

As can be seen in Figure 1, a small water buffer tank is present in the hydronic loop for each configuration in order to increase the thermal inertia of the system. The buffer tank is a commercial 79 liters water storage having a well-insulated blanket (U-value equal to 0.8 W/m^2K). The considered thermal storage allows to limit the frequency of the heat pump on-off cycles under 6 start-ups per hour, which is the maximum value recommended by the heat pump manufacturer.

Each thermal zone is heated by a single terminal unit, sized on the design load of the room. The emitters are low-temperature radiators, each one equipped with a thermostatic valve. The design supply temperature $T_{w,des}$ (i.e. the supply water temperature in correspondence of the design outdoor temperature T_{des}) has been set equal to 55°C and the design water flowrate has been calculated for each radiator by fixing a nominal temperature difference of 10 K. Moreover, the set-point temperature of the supply hot water to the emitters ($T_{w,set}$) is variable during the heating season and depends on the outdoor air temperature: in each configuration the heat generator produces hot water at the same temperature as the value given by the climatic curve reported in [34].

A by-pass valve guarantees the effectiveness of the variable flow rate emitters and ensures the correct operation of the constant-speed circulating pump. In fact, the hot side water flow is split between the emitters and the by-pass loop according to the thermostatic valve opening,

The boiler used in these simulations is a condensing gas-fired unit. The dynamic model of this device is based on a performance-map approach: the performance data of a commercial boiler, as reported by the technical datasheets of the manufacturer, have been used to build the look-up table introduced in the model. The main technical characteristics of the selected unit are reported in Table 1 and the boiler efficiency referred to the Lower Heating Value (LHV), η_g, is shown in Figure 2 as a function of the part load factor, φ, and of the return water temperature, $T_{w,in}$. Reported data highlight that the boiler is characterized by an efficiency larger than 1 only for load factors lower than 0.70.

Table 1. Condensing boiler technical data.

Parameter	Value
Nominal heating capacity (supply/return water temperature = 80/60°C)	21.5 kW
Nominal η_g (supply/return water temperature = 80/60°C)	97.5%
Heating capacity modulation range	[0.25-1.00]
$\tau_{on,h,B}$	125 s
$\tau_{off,h,B}$	0 s

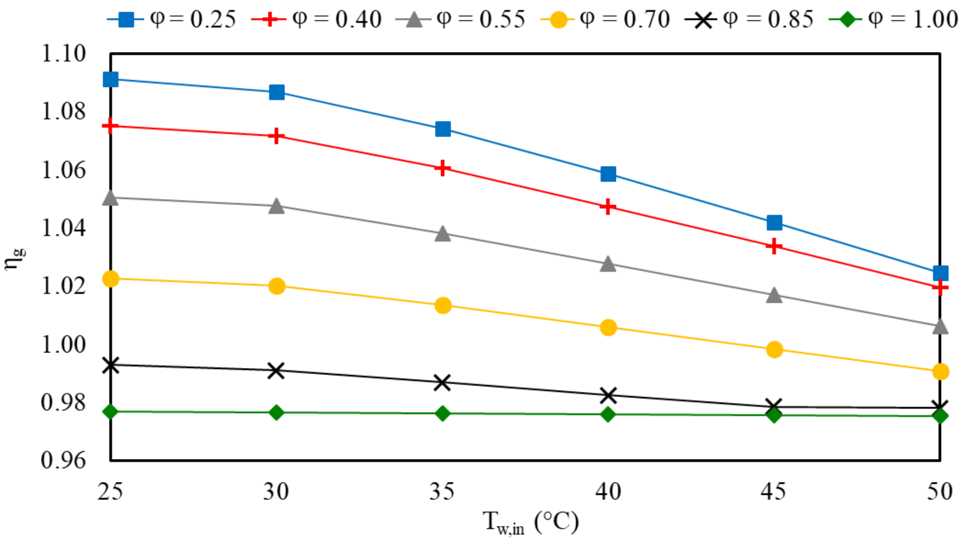

Figure 2. Boiler efficiency as a function of return water temperature and part load factor.

The energy losses linked to the boiler on-off cycles have been taken into account: although the unit is characterized by a broad modulation range ([0.25-1.00], see Table 1), when the building heating load is very low, on-off cycles must be performed by the boiler and its efficiency decreases due to the heat losses from the generator casing and the exhaust gases [30]. Following the methodology described by Dongellini and Morini [33], the boiler start-up losses have been considered by introducing an exponential corrective factor for the boiler heating capacity during the start-up transient. The time constant of this phase ($\tau_{on,h,B}$) has been evaluated experimentally by the boiler manufacturer and its value is reported in Table 1. Similarly, the boiler behavior during the shut-down transient has been evaluated but, in this case, the delivered heating power becomes zero when the device is switched off and no recovery effects are considered. For this reason, the time constant of the shut-down transient ($\tau_{off,h,B}$) is set equal to zero.

Table 2. Technical data of the selected air-to-water inverter-driven heat pump

Parameter	Value
Nominal heating capacity (T_{ext} = 7°C, supply/return water temperature = 55/45°C)	14.7 kW
Nominal *COP* (T_{ext} = 7°C, supply/return water temperature = 55/45°C)	2.13
Refrigerant	R410A
Compressor data	Twin rotary variable speed device (frequency range: 15-115 Hz)
$\tau_{on,h,HP}$	35 s
$\tau_{off,h,HP}$	0 s
$\tau_{on,ee,h,HP}$	10 s
$\tau_{off,ee,h,HP}$	0 s

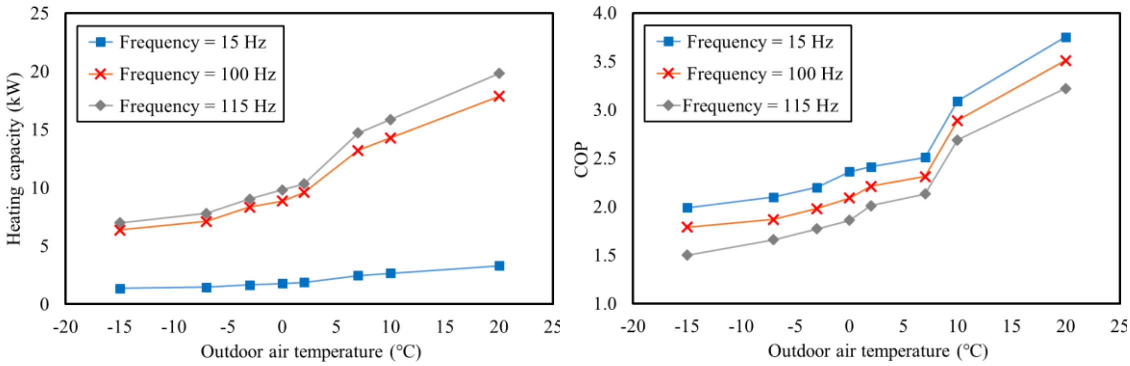

(a) (b)

Figure 3. Full load and partial load heat pump performance data for water supply/return temperature equal to 55/45°C: heating capacity (a) and COP (b) as functions of the outdoor air temperature.

The AWHP unit considered in the simulations is an inverter-driven heat pump based on a compression cycle. The unit has been modelled by using a performance-map approach, as described in [33]. The heat pump heating capacity and *COP* are evaluated by means of a three-dimensional look-up table as a function of the inverter frequency, Φ, and of the sink and source temperatures (i.e. return water temperature, $T_{w,in}$ and external air temperature, T_{ext}, respectively). These data have been obtained by a series of experimental measures made in collaboration with the heat pump manufacturer. In Table 2 and Figure 3 the main technical data, and the full load and partial load performance data of the modelled heat pump are reported, respectively.

Since the AWHP is sized on the building design load, the unit modulates its delivered thermal capacity during the milder part of the season to meet the building energy demand. For this reason, the heat pump carries out a significant number of on-off cycles when a further modulation of the compressor speed is not possible (i.e. in correspondence of the hottest part of the heating season). The energy losses linked to the heat pump on-off cycling have been taken into account by using the model described in [33]: the energy performance of the unit is reduced at each start-up because the pressure difference between high- and low-pressure sides must be restored. This degradation effect consists on a reduction of the unit heating capacity, rather than on an increase of the electrical power input [35]: experimental tests conducted in collaboration with the heat pump manufacturer allowed to measure the duration of the start-up transient and to evaluate the characteristic time constants of the heat pump ($\tau_{on,h,HP}$, $\tau_{off,h,HP}$, $\tau_{on,ee,h,HP}$, $\tau_{off,ee,h,HP}$), whose values are reported in Table 2. It is important to highlight that the unit considered in this work is equipped with an Electronic Expansion Valve (EEV), which guarantees lower cycling losses with respect to a Thermostatic Expansion Valve (TEV), as highlighted in [15].

Since the most widespread defrosting strategy for air-source heat pumps is the reverse cycle method [36], a simplified model based on this technique, able to take into account frost formation and defrosting energy losses, has been used in this work. Full details about this simplified model can be found in Vocale et al. [37]. When a defrost cycle is performed, the unit outdoor heat exchanger operates as a condenser and the indoor heat exchanger acts as an evaporator. Before the cycle inversion, the heat pump is switched off for about 1 minute: during this period the outdoor fans are stopped and the four-way valve is reversed. After this stand-by period the unit operates in cooling mode and the frost layer is melted. Finally, after another stand-by period (1 minute) the four-way valve reverses again and the heat pump returns to the heating operating mode. The duration of the defrost cycle typically ranges from 90 seconds to 8 minutes ([38]-[40]) and it is defined by the heat pump controller. In this work each defrost cycle runs for 7 minutes (1 minute for the first stand-by period, 5 minutes for the cooling reversed mode and 1 minute for the second stand-by period). Defrost cycles are performed by the heat pump regularly at defined intervals: when the outdoor air temperature is below 5°C and at the same time the relative humidity is above 75%, a defrost cycle is repeated each 45 minutes.

In the HHP configurations shown in Figure 1c and in Figure 1d, the heat pump and the back-up heat generator are connected in series and can operate independently of one another. The control system continuously monitors the temperature of the hot water supplied by the heat pump and compares it with a set-point value: when the heat pump heating capacity is lower than the building thermal load, the back-up device is switched on. In the following Sections, further details on the system control algorithms will be given.

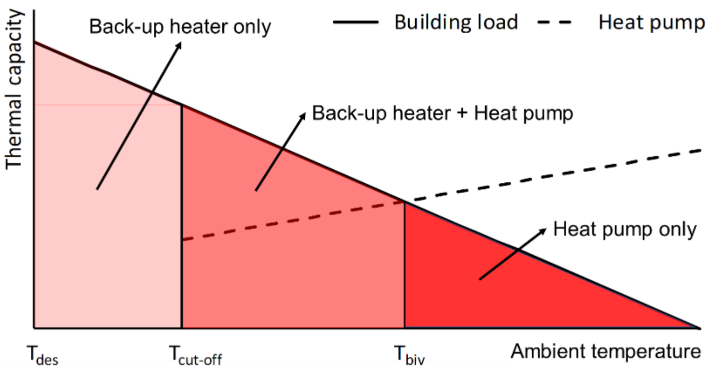

Figure 4. Main parameters and possible operating modes of a hybrid heat pump system.

In Figure 4 the operating modes and the main parameters related to HHP systems are presented. The bivalent temperature (T_{biv}) is shown in Figure 4 in correspondence of the point in which the building heating load (solid line) equals the heat pump heating capacity (dashed line).

Another parameter used for the analysis of this kind of systems is the peak load ratio, β~~,~~. This parameter is defined in Eq. 1 as the ratio between the heat pump heating capacity at design conditions (P_{HP} (T_{des})), and the building peak load (P_{des}):

$$\beta = \frac{P_{HP}(T_{des})}{P_{des}} \tag{1}$$

For monovalent systems based on an AWHP only, the peak load ratio is equal to or larger than 1. In HHP systems, β ranges from 0 to 1: the higher the heat pump size, the higher the peak load ratio.

In addition, the cut-off temperature ($T_{cut\text{-}off}$) is here defined as the value of the ambient temperature in correspondence of which the heat pump is switched off due to specific control rules, typically related to energetic or economic considerations. When the outdoor air temperature is below the cut-off temperature, the back-up device is the only active heat generator.

If $T_{cut\text{-}off} = T_{biv}$, the hybrid system operates by switching on the back-up heater and switching off the heat pump when $T_{ext} < T_{biv}$. In this case, the heating system works in pure alternative mode. On the other hand, if the control system sets a cut-off temperature lower than the bivalent temperature, both heat generators are switched on when $T_{cut\text{-}off} < T_{ext} < T_{biv}$: in this case the heat generators operate in parallel. Furthermore, a pure parallel configuration is set if $T_{cut\text{-}off}$ is fixed equal to the design temperature, T_{des}. In this case the heat pump is active during the whole heating season, even for low values of the outdoor temperature.

2.2. Building modeling and climatic data

The residential building SFH100 described by the report IEA SHC Task 44/HPP Annex 38 (T44A38) [34] has been considered as reference case study. The considered building is characterized by a net heated volume of about 390 m^3 and a heated floor area of 140 m^2. It represents a non-renovated existing house: the UA-value of the entire building is 290 W/K and its heating demand is equal to 100 kWh/(m^2 y) for the climate of Strasbourg. Simulations have been performed for the Italian climate of Bolzano, a location placed in the North of Italy and characterized by a cold and humid winter. According to current Italian law [41], the heating system is switched on from October, 15th to April, 15th, for a total of 183 days. The simulation timestep has been set equal to 30 s, in order to avoid numerical and convergence issues.

The Typical Meteorological Year (TMY) of Bolzano reported within the TRNSYS weather data library has been used to obtain the hourly climatic data: according to this data, the design outdoor air temperature, T_{des}, is equal to -9°C, while the heating degree days (HDDs) over the heating season, calculated with a base temperature of 20°C, are 2656. Furthermore, the heat generator operates 24/7 along this period and the internal set-point temperature is set to 20°C along the whole season, with no night set-back.

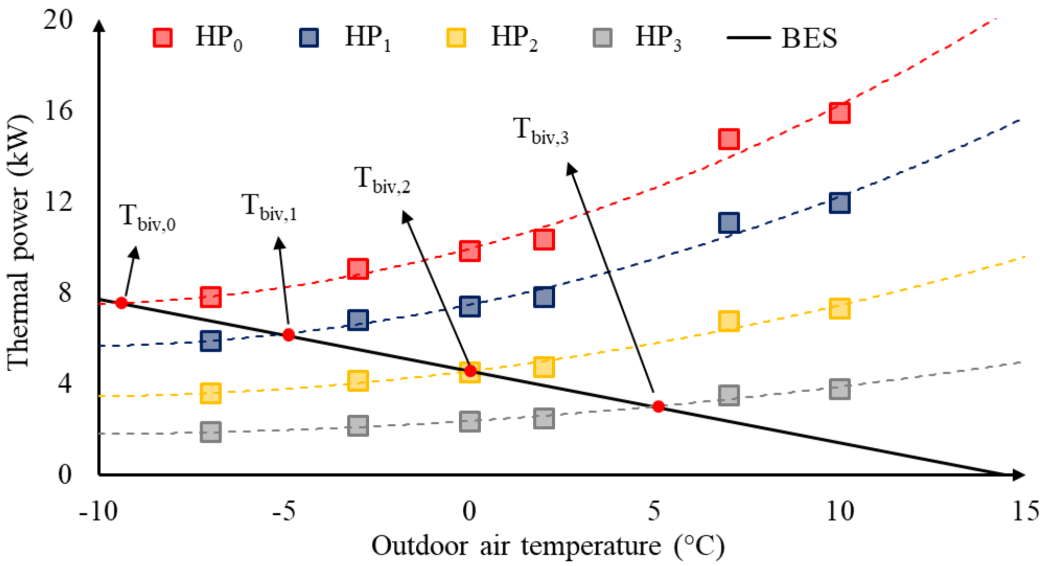

Figure 5. Performance data at full load of the considered heat pumps and building energy signature (BES)

The heat load of the building has been calculated by means of the TRNBUILD plugin of TRNSYS [42]: in correspondence of the design ambient temperature (i.e. -9°C for Bolzano) the design load of ground floor and first floor is equal to 3.11 and 4.27 kW, respectively, corresponding to a peak load for the heat distribution system of 7.38 kW. Moreover, according to the building energy signature method (BES) [43], the thermal load required by the building during the heating season has been correlated to the external air temperature by means of a linear function: in Figure 5 the BES of the reference building is shown with a solid black line. It is evident that the required thermal load vanishes for outdoor temperatures higher than 15°C due to internal and solar heat gains.

2.3. Heating system configurations

Table 3. Performance data of the simulated heating systems (heat pump data evaluated for supply/return water temperatures equal to 55/45°C)

Case	#1	#2	#3	#4	#5	#6	#7	#8
Heat generators	HP_0	HP_1+ER	HP_2+ER	HP_3+ER	HP_1+B	HP_2+B	HP_3+B	B
T_{biv} (°C)	-10	-5	0	+5	-5	0	+5	/
P_{HP} (T_{des}) (kW)	7.52	5.48	3.34	1.65	5.48	3.34	1.65	/
P_{bu} (kW)	/	1.90	4.04	5.73	21.5	21.5	21.5	/
β	1	0.74	0.45	0.22	0.74	0.45	0.22	0

In order to study the influence of the heat pump size on the seasonal energy performance of a HHP system, four air-to-water heat pumps (HP) have been considered in this work, coupled to electric resistances (ER) or to a gas-fired boiler (B). The main characteristics of the simulated units are summarized in Table 3.

In Figure 5 the heating capacity at full load of the heat pumps is reported as a function of the ambient temperature by fixing inlet/outlet water temperatures equal to 45/55°C, respectively. In that Figure, the heat pump used in the monovalent system has been referred to as HP_0, while the smaller units used in HHP systems have been indicated as

HP_1, HP_2 and HP_3, respectively. In addition, in Figure 5 and in Table 3 the bivalent temperature of each configuration, T_{biv}, is also shown. It is evident that by scaling from HP_0 to HP_3 the value of T_{biv} strongly increases and, for this reason, the peak load ratio, β, decreases. As a consequence, when undersized heat pumps are considered, the back-up heater heating capacity, P_{bu}, increases in order to completely satisfy the building energy demand. When an electric resistance is used as back-up unit in a HHP system, its rated capacity is calculated as the difference between the building peak load and the heat pump heat supply at design conditions. On the other hand, the condensing gas boiler considered as back-up device in configurations #5-#7 is the same gas-fired unit described in Section 2.1 and used as single heat generator in the reference configuration shown in Figure 1a.

It is important to highlight that when the heat pump size decreases, passing from HP_0 to HP_3, the peak load ratio decreases from 1 to 0.22 (see Table 3): when the smallest unit is considered, almost 80% of the building peak load at design conditions is satisfied by the back-up heater. The peak load ratio is related to the bivalent temperature of the system, which is equal to -5°C, 0°C and +5°C when HP_1, HP_2 and HP_3 are respectively considered for HHP systems, and is lower than the design temperature for the reference heating system based on HP_0.

2.4. Control strategies of the heating systems

The gas boiler control logic is based on a PI controller coupled to an on-off algorithm. The flow chart of the boiler control strategy is shown in Figure 6a, as a reference. As long as the boiler load factor φ is between the declared modulating range reported in Table 1 (i.e. between 1 and 0.25), the boiler heating capacity is modulated to maintain the supply water temperature equal to its set-point value, fixed by the climatic curve and depending on the current ambient temperature.

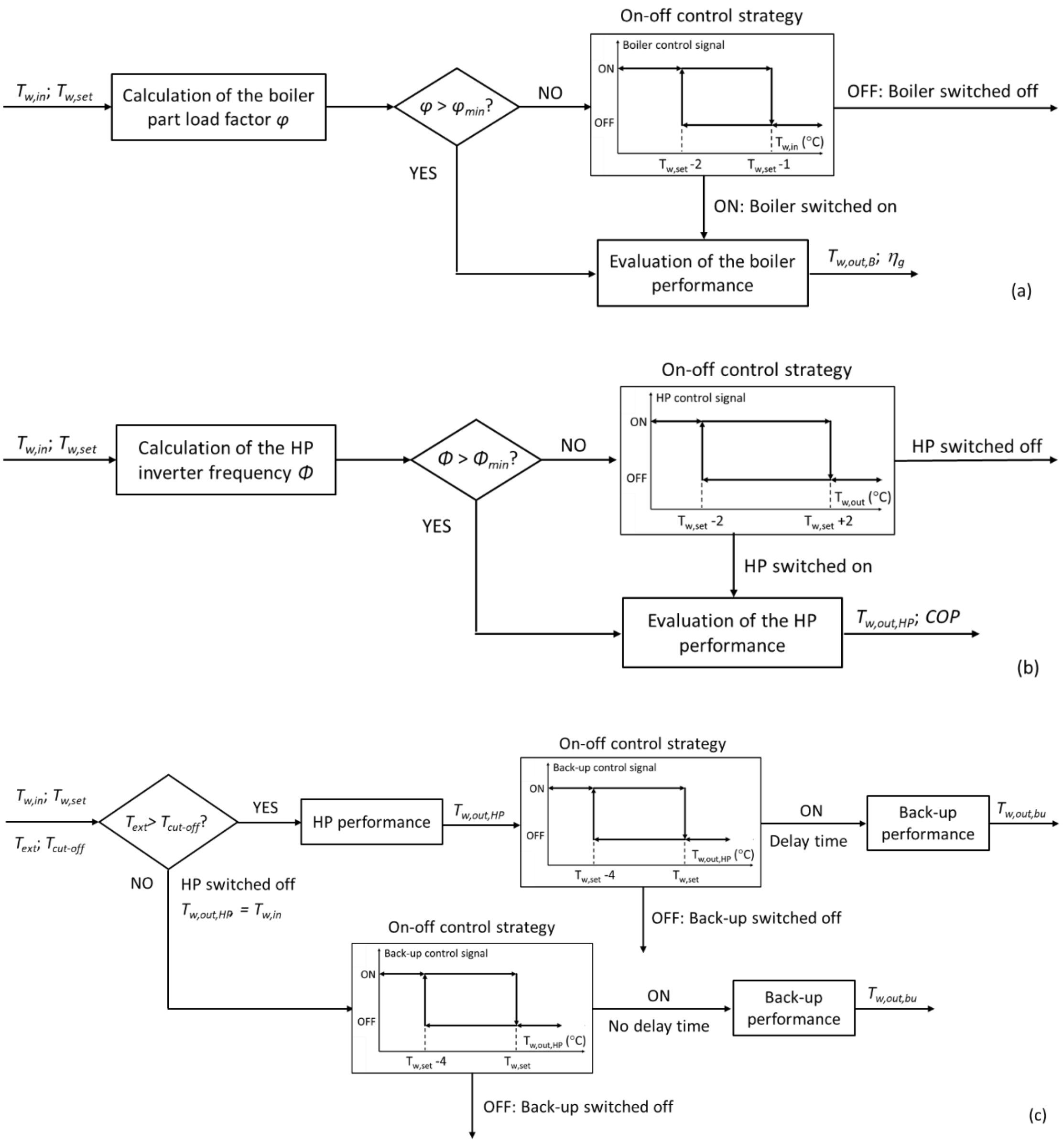

Figure 6. Control algorithm implemented in TRNSYS for the gas boiler (a), the AWHP (b) and the hybrid system configurations (c)

On the other hand, when the device delivers the minimum thermal power and no further modulation is possible, the unit performs a series of on-off cycles to balance the building heat load. The monitored variable during this operating mode is the return water temperature, $T_{w,in}$: the boiler is switched off when $T_{w,in}$ becomes higher than $T_{w,set}$ - 1 K and it is then switched on when $T_{w,in}$ is lower than $T_{w,set}$ - 2 K. The dead-band is needed to prevent frequent oscillations of the boiler control signal and to limit the unit cycling frequency.

As illustrated in Figure 6b, the heat pump control strategy is similar to that of the boiler: a PI controller is adopted to set the inverter frequency and an on-off logic is activated during the milder part of the season when the minimum frequency is reached. The heat pump control system uses the supply water temperature at the outlet of the unit ($T_{w,out,HP}$) as monitored variable and compares it to the set-point value imposed by the climatic curve. By means of the PI algorithm, the inverter frequency is set to adapt the heat pump heating capacity to the building heat load. For each unit considered in this work, the PI parameters have been fixed to the same values: proportional gain K_p and integral time t_i have been set to 5 and 300 s, respectively. As pointed out by the technical data reported in Table 2, the inverter modulation range broadens from 15 Hz to 115 Hz. When the building energy demand is low and the minimum frequency is reached, the heat pump operates as a fixed-speed unit and the on-off control logic is introduced. This on-off algorithm is characterized by a hysteresis cycle of amplitude 4 K centered around the supply water set-point temperature. $T_{w,set}$. The adopted dead-band allows to reduce the oscillations of the heat pump control signal, lowering both energy losses and compressor mechanical stress.

On the other hand, HHP systems (i.e. cases #2 - #7 in Table 3) are characterized by two devices which have to be independently activated. The back-up heater control strategy has to satisfy several constraints in order to avoid energy losses and guarantee thermal comfort for building users:

1. for parallel operating mode (i.e. when $T_{cut\text{-}off} < T_{ext} < T_{biv}$) the back-up device is switched on only when the heat pump is activated and its heating capacity is lower than the building load;
2. the back-up device has to limit its on-off cycle frequency;
3. a fixed delay for the back-up generator activation must be introduced to avoid unnecessary operations, for example after a heat pump defrost cycle.

In Figure 6c the detailed flow chart of the control algorithm implemented for HHP systems is shown. The back-up device control logic uses the water temperature at the outlet of the heat pump as monitored variable and is characterized by an on-off control strategy based on a hysteresis cycle: the back-up heater is activated when $T_{w,out,HP}$ is 4 K lower than the supply water set-point temperature ($T_{w,set}$) and is then switched off when $T_{w,out,HP}$ returns higher than $T_{w,set}$.

As stated previously, the back-up heater is not directly activated when the water temperature at the heat pump outlet starts to decrease: a delay time, t_{del}, equal to 15 minutes has been introduced before the activation of the back-up system. This value has been set in order to obtain the best compromise between two opposite aspects: energy consumptions of the system and indoor comfort conditions. In fact, with a short delay time, the back-up heater would be switched on even if unnecessary, maintaining optimal comfort conditions within thermal zones but with larger energy consumptions; on the contrary, the increase of the delay time causes a worsening of indoor thermal comfort, since the back-up device would be activated when the supply water temperature is far below its set-point value.

Finally, when the pure alternative or the alternative-parallel operating mode are activated, a further control logic has been implemented. For configurations #5 - #7 (see Table 3), characterized by a gas boiler as back-up device, the cut-off temperature ($T_{cut\text{-}off}$) is introduced: when the outdoor temperature is lower than $T_{cut\text{-}off}$, the heat pump is completely disabled and no delay time is considered for the activation of the boiler. On the contrary, when T_{ext} is between $T_{cut\text{-}off}$ and T_{biv}, both heat generators are activated: in this case the back-up heater is activated with the delay time of 15 minutes previously introduced.

In this study, different values of $T_{cut\text{-}off}$ have been considered in order to assess the influence of the control strategy on the energy performance of HHP systems; for each configuration, a series of simulations has been performed, defining five cut-off temperatures ranging from the outdoor design temperature (i.e. -9°C) and an upper limit fixed to 5°C.

2.5. Key performance indicators

In order to evaluate the seasonal efficiency of HHP systems in which different heaters (i.e. boilers, heat pumps and electric resistances) are fed with different energy vectors (i.e. electric energy (*ee*) and natural gas (*gas*)), and with the aim to compare the seasonal energy performance of all the considered configurations, the system seasonal efficiency, η_S, has been defined in Eq. 2 as the ratio between the total amount of thermal energy supplied by the heating system to the building, $E_{th,tot}$, and the total primary energy consumption of the system, $E_{p,tot}$:

$$\eta_S = \frac{E_{th,tot}}{E_{p,tot}} = \frac{\sum_j E_{th,j}}{\sum_j \sum_i E_{p,i,j}} \text{ with j=}B, ER, HP \text{ and i= } ee, gas \qquad (2)$$

where $E_{th,j}$ and $E_{p,i,j}$ are the thermal energy supplied to the building by the j-th heater along the season and the seasonal primary energy demand of the j-th heater linked to the i-th energy vector, respectively. Furthermore, $E_{p,i,j}$ is calculated starting from the seasonal energy consumption of the j-th heat generator linked to the i-th energy vector ($E_{i,j}$), multiplied for the corresponding primary energy conversion factor (PEF_i), as shown in the following Equation:

$$E_{p,i,j} = E_{i,j} PEF_i \text{ with j=B, ER, HP and i= } ee, gas \qquad (3)$$

The values of PEF_i fixed by Italian law [44] for electric energy and natural gas are equal to 2.42 and 1.05, respectively; these values have been used in the analysis presented in this work.

A series of additional performance indicators can be associated to the single heaters of HHP systems; for the heat pump, the condensing gas boiler and the electric heater, the $SCOP_{net}$, the seasonal boiler efficiency η_B and the electric heater efficiency η_{ER} are introduced in Eqs. 4, 5 and 6, respectively

$$SCOP_{net} = \frac{E_{th,HP}}{E_{HP,ee}} \qquad (4)$$

$$\eta_B = \frac{E_{th,B}}{E_{B,gas}} \qquad (5)$$

$$\eta_{ER} = \frac{E_{th,ER}}{E_{ER,ee}} \tag{6}$$

For the electric heater, a seasonal efficiency equal to 1 is assumed.

The methodology reported by the European standard EN 14825 [45] has been used to evaluate the heat pump seasonal coefficient of performance, $SCOP_{net}$, for heating systems based on a heat pump (i.e. configurations #1 - #7 of Table 3). Following EN 14825 for HHP systems with a back-up based on an electric heater (i.e. configurations #2 - #4 in Table 3), the heating seasonal coefficient of performance of the system, *SCOP*, is here ~~introduced~~defined as:

$$SCOP = \frac{E_{th,HP} + E_{th,ER}}{E_{HP,ee} + E_{ER,ee}} \tag{7}$$

3. RESULTS AND DISCUSSION

In order to investigate the influence of back-up heater typology and heat pump size on the seasonal energy efficiency of the whole system, a first series of simulations has been performed selecting the cut-off temperature of HHP systems equal to the outdoor design temperature for all cases. Therefore, for hybrid configurations, both heaters are activated in parallel during the whole heating season with priority on the heat pump, considered as the main heater of the system. Moreover, in these simulations both the defrost and cycling losses have been considered.

In Figure 7 the thermal energy supplied to the building by the whole heating system ($E_{th,tot}$) and the total primary energy consumption ($E_{p,tot}$) are reported for the simulated cases. Moreover, the thermal energy supplied to the building by both the back-up device and the main heater (i.e. $E_{th,bu}$ and $E_{th,gen}$, respectively) is shown in the same figure as well. It is important to highlight that $E_{th,bu}$ is equal to $E_{th,ER}$ for cases #2 - #4 and to $E_{th,B}$ for cases #5 - #7, while $E_{th,gen}$ corresponds to $E_{th,HP}$ for cases #1 - #7 and to $E_{th,B}$ for case #8. Obviously, $E_{th,gen}$ corresponds also to $E_{th,tot}$ for cases #1 and #8, since the heat pump and the boiler are the only heat generators in these configurations.

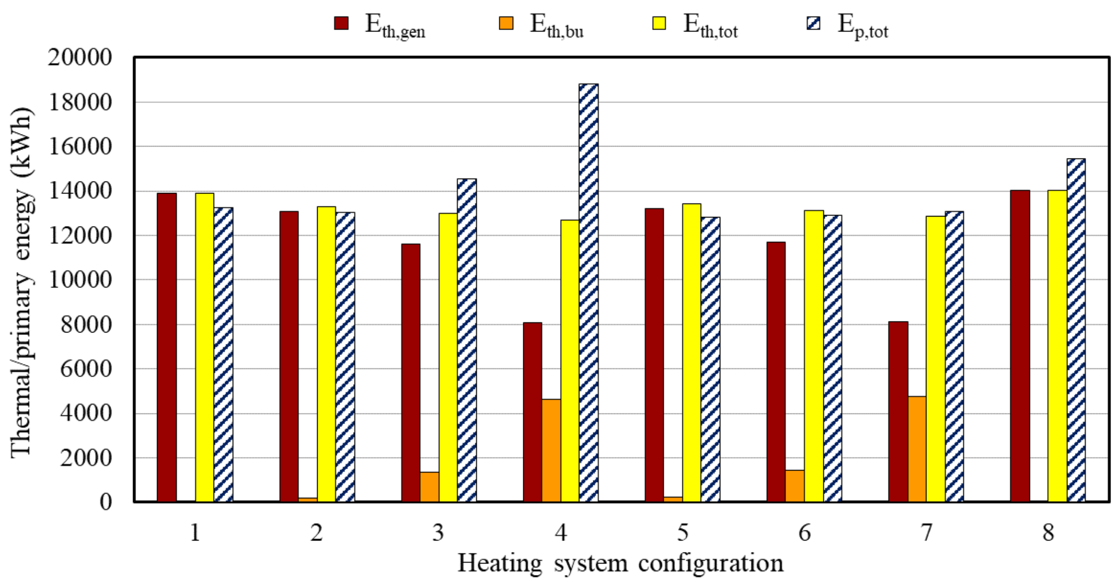

Figure 7. Thermal energy delivered to the building by the main heater and by the back-up device and primary energy consumption of the system

The reference system based on the single heat pump as heater (HP_0, case #1) is able to guarantee a lower primary energy consumption with respect to the condensing gas boiler (case #8). This quantity is slightly reduced when HHP systems are used in presence of both electric heaters (case #2) and gas boilers (case #5, #6 and #7) as back-up devices. These results confirm the conclusion made by Klein et al. [29], for which the maximum efficiency of HHP systems is achieved with heat pumps sized to cover only a fraction of the design load. If an electric heater is used as back-up, the heat pump has to be sized in order to cover at least 70% of the design heat load in order to minimize the total primary energy consumptions. On the contrary, smaller heat pumps (down to 40% of the design thermal load) can be adopted if a boiler is used as back-up unit.

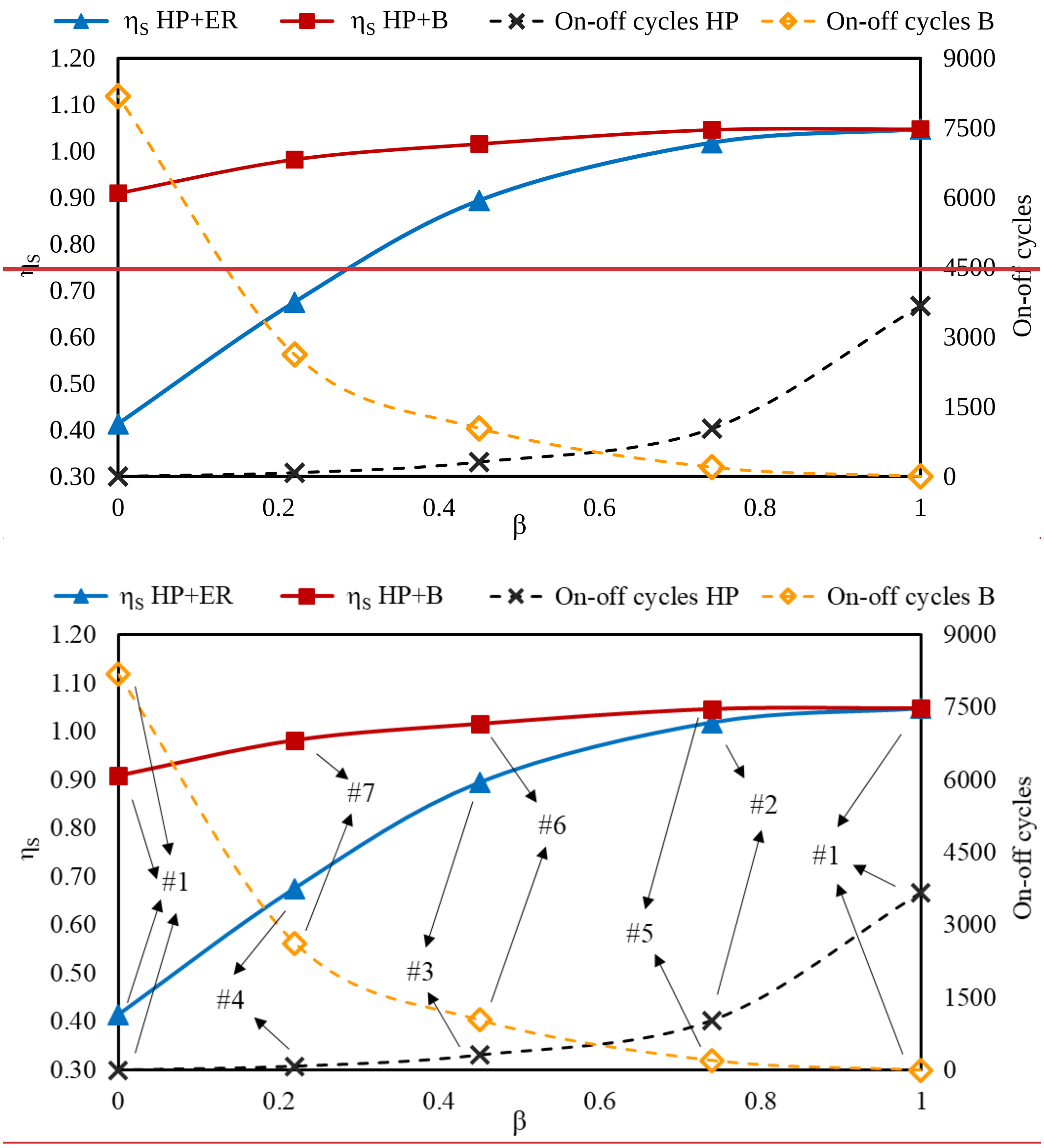

Figure 8. Seasonal energy efficiency of the system, heat pump and boiler seasonal on-off cycles as functions of the building peak load ratio

In Figure 8 the seasonal energy efficiency of the system, η_S, and the total number of on-off cycles carried out by the heat pump and the boiler are shown as functions of the building peak load ratio for all the simulated cases. It is evident from Figure 8 that when the size of the heat pump is reduced with respect to the design heat load, the number of on-off cycles performed by the heat pump is strongly reduced, decreasing from 3666 cycles for case #1 to 80 cycles for cases #4 and #7 (-98%). Indeed, with undersized heat pumps, on-off cycling must be used to adapt the unit heating capacity to the building heat load only in the milder part of the heating season. The number of on-off cycles carried out by the heat pump is independent from the typology of back-up unit: as a consequence, when undersized devices are used in HHP systems, the energy losses linked to on-off cycles are reduced and, for this reason, the energy performance of the heat pump is improved. Nevertheless, the considered heat pumps are equipped with an EEV: since with this kind of expansion valves the energy penalization linked to each on-off cycle is low, the enhancement of the heat pump seasonal performance is significant only for units characterized by a peak load ratio lower than 0.5. On the contrary, the number of defrost cycles performed by the heat pump does not change since the control strategy for the activation of the defrosting transient depends on the outdoor conditions and the parameters of its algorithm are the same for each case. Results point out that, in fact, the heat pumps used as main generator in cases #1 - #7 carry out the same number of defrost cycles along the heating season (1491) and, for this reason, the impact of defrosting energy losses on η_S has the same order of magnitude for all pure parallel configurations. As it will be reported in detail in a following section of the paper, the seasonal efficiency of the system has a penalty larger than 7% due to defrost cycles.

Furthermore, in order to satisfy the building required load, the smaller heat pumps are called to operate at larger inverter frequency with respect to the heat pumps sized on the building peak load (case #1) and, as pointed out by Figure 3, their seasonal *COP* values are lower.

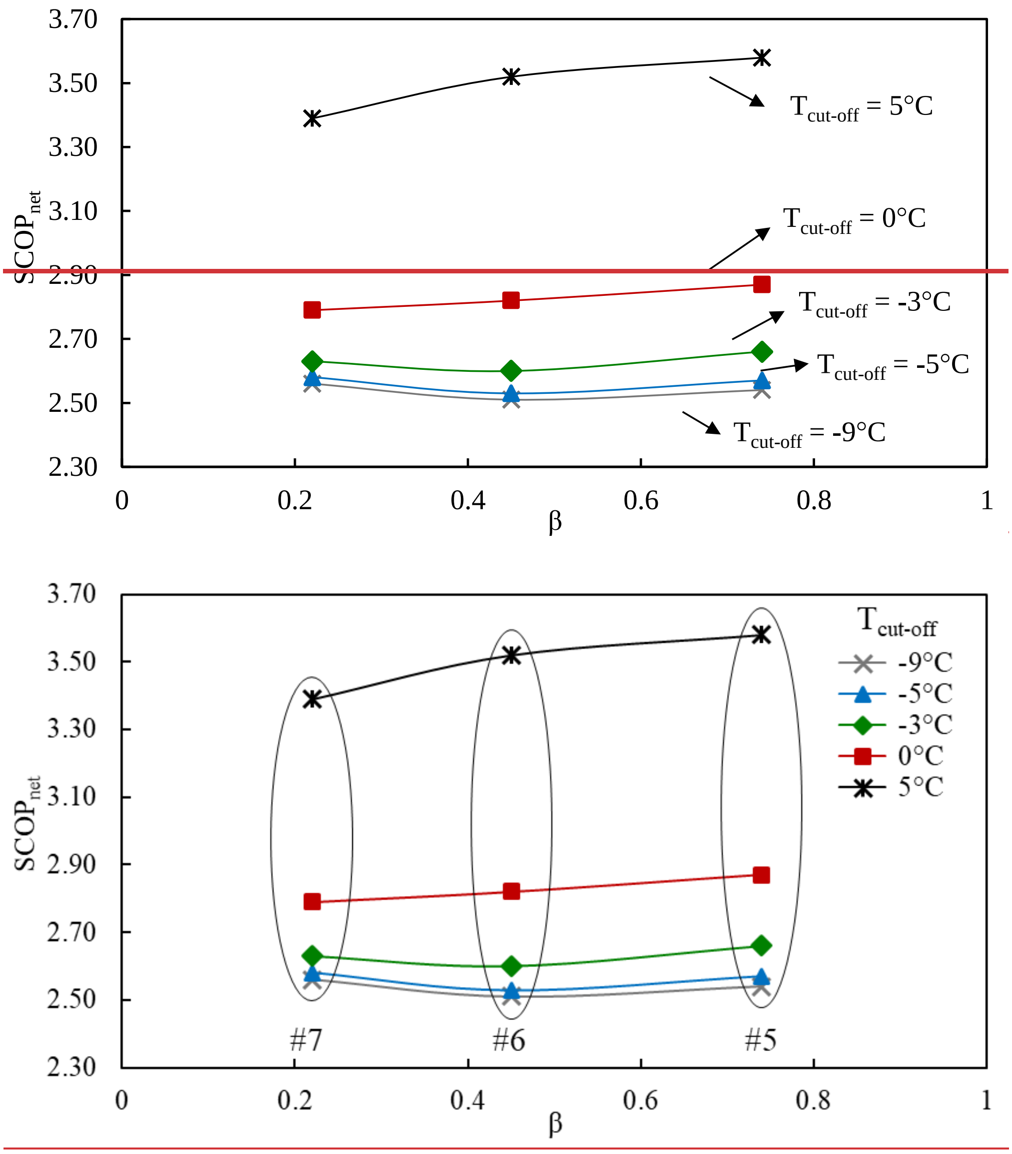

3.70
3.50
3.30
3.10
2.90
2.70
2.50
2.30
SCOP$_{net}$
0
0.2
0.4
0.6
0.8
1
β
T$_{cut-off}$ = 5°C
T$_{cut-off}$ = 0°C
T$_{cut-off}$ = -3°C
T$_{cut-off}$ = -5°C
T$_{cut-off}$ = -9°C
T$_{cut-off}$
-9°C
-5°C
-3°C
0°C
5°C
#7
#6
#5

(a)

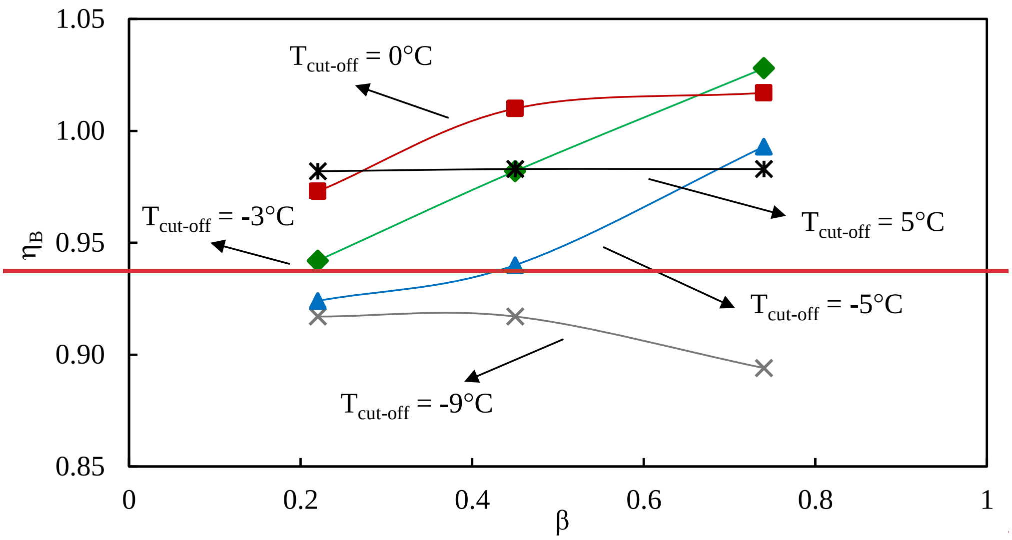

1.05
1.00
0.95
0.90
0.85
η_B
$T_{cut-off}$ = 0°C
$T_{cut-off}$ = -3°C
$T_{cut-off}$ = 5°C
$T_{cut-off}$ = -5°C
$T_{cut-off}$ = -9°C
0
0.2
0.4
0.6
0.8
1
β

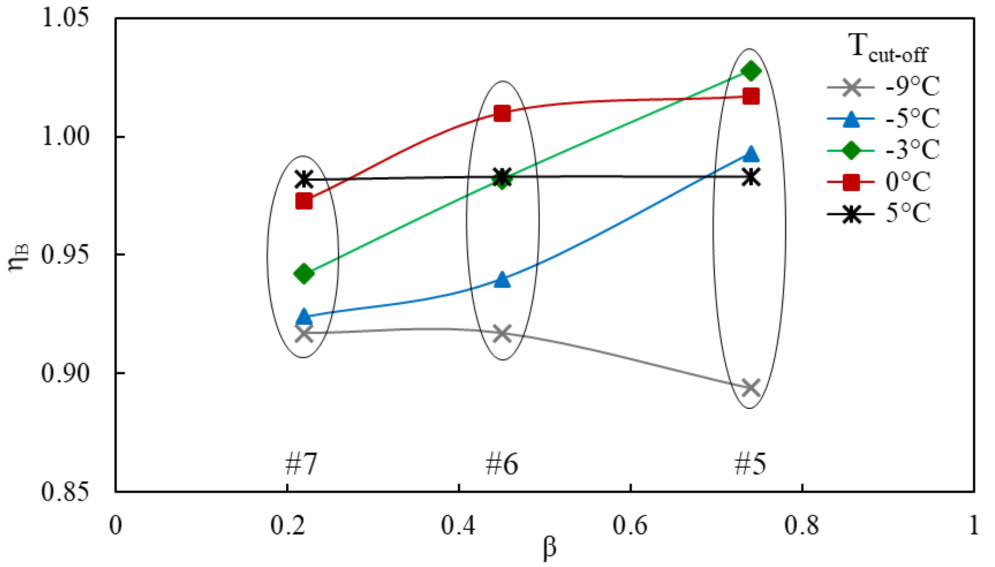

1.05
1.00
0.95
0.90
0.85
η_B
$T_{cut-off}$
-9°C
-5°C
-3°C
0°C
5°C
#7
#6
#5
0
0.2
0.4
0.6
0.8
1
β

(b)

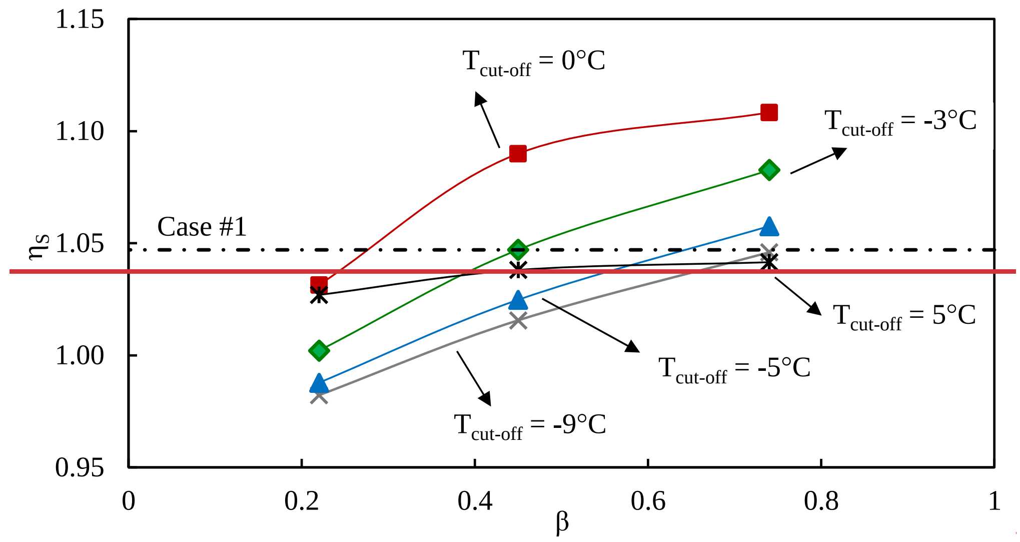

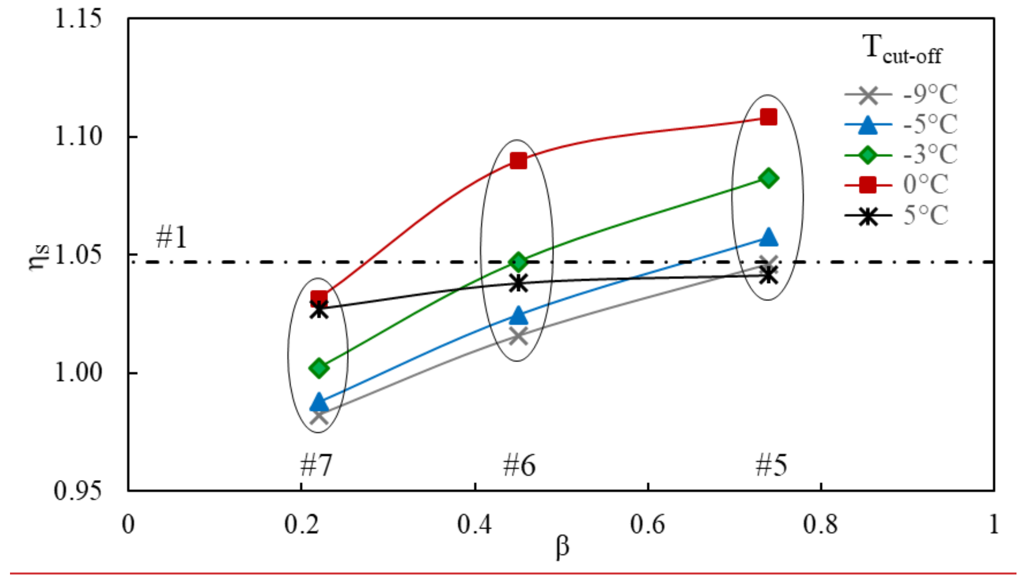

(c)

Figure 9. Seasonal energy performance indicators of the studied systems as functions of the peak load ratio and of the cut-off temperature: $SCOP_{net}$ (a), η_B (b) and η_S (c)

A second series of simulations was focused on the role played by the choice of the cut-off temperature on the seasonal energy performance of HHP systems fed by two energy vectors (i.e. case #5, #6 and #7, with a gas boiler as back-up heater). The seasonal efficiency of the system has been calculated for different values of the cut-off temperature and compared to that obtained for case #1 (i.e. a monovalent system based on the heat pump HP_0): Figure 9 highlights the influence of $T_{cut\text{-}off}$ and of the peak load ratio, β, on the seasonal energy performance indicators of the system (i.e. $SCOP_{net}$, η_B and η_S, see Eqs. 4, 5 and 2, respectively).

Figure 9 shows that significant primary energy savings can be obtained by adopting an alternative hybrid system configuration if compared to conventional monovalent heating systems based on an AWHP or a condensing gas boiler. Moreover, there exists for each specific application an optimal configuration of the HHP system for which η_S assumes its maximum value. In our case study, the largest value of η_S is obtained for β=0.74 (case #5), setting the cut-off temperature equal to 0°C. Under these conditions, the seasonal efficiency of the heating system can be enhanced up to +6% and +22% with respect to the reference cases #1 and #8, in which a single heat generator is used (i.e. an AWHP and a condensing gas boiler, respectively). Moreover, it is evident from Figure 9c that a similar trend of η_S as a function of the cut-off temperature is obtained for all the values of the peak load ratio. Indeed, in the present study, for each value of the bivalent temperature, η_S increases when $T_{cut\text{-}off}$ increases and presents a maximum in correspondence of 0°C. However, the optimal value of the cut-off temperature depends on the climatic conditions of the site and in presence of mild winter conditions (in terms of both outdoor air temperature and humidity) can shift towards the design temperature, which means heat pump active for a longer time.

The energy performance results can be fully explained by observing Figure 9a and Figure 9b, in which the values of $SCOP_{net}$ and η_B are respectively shown as functions of the peak load ratio and of the cut-off temperature. First, it is evident that for each heat pump size (i.e. for all values of β) the seasonal energy performance of the unit monotonically increases when the cut-off temperature increases. In fact, when the heat pump size is reduced, its $SCOP_{net}$ is improved for two reasons: i) when $T_{cut\text{-}off}$ increases, the number of defrost cycles performed by the heat pump decreases, as will be highlighted in a following figure; ii) the period in correspondence of which the heat pump operates with low *COP* values, due to low external temperatures and large compressor frequency, is strongly reduced.

It is important to stress that when the peak load ratio is decreased, an increasing share of the building heat demand is supplied by the back-up boiler and, for this reason, the energy performance of the whole HHP system is more influenced by the boiler seasonal efficiency. As reported by Figure 9b, η_B is characterized by different trends when the peak load ratio decreases: for each configuration, the boiler seasonal efficiency has its maximum value in correspondence of a cut-off temperature close to the corresponding bivalent temperature (-3°C, 0°C and 5°C for cases #5, #6 and #7, respectively). In all cases, η_B is characterized by a monotonic increasing trend when $T_{cut\text{-}off}$ is lower than T_{biv}: when the cut-off temperature increases, the HHP system operates for a longer time in alternative mode (i.e. with the back-up as the unique active heat generator) and the boiler performance becomes more and more influent on the system overall efficiency.

In Figure 10a the annual number of defrost and on-off cycles performed by the air-to-water heat pumps are reported as functions of the cut-off temperature and of the peak load ratio. It is evident that the higher the cut-off temperature, the lower the number of defrost cycles carried out by the heat pump. For example, when $T_{cut\text{-}off}$ is set equal to 0°C, the number of defrost cycles is reduced up to 47% with respect to pure parallel configurations (i.e. $T_{cut\text{-}off}$ equal to T_{des}), while defrosting energy losses can be completely avoided in the site considered in these simulations for $T_{cut\text{-}off}$ equal to 5°C.

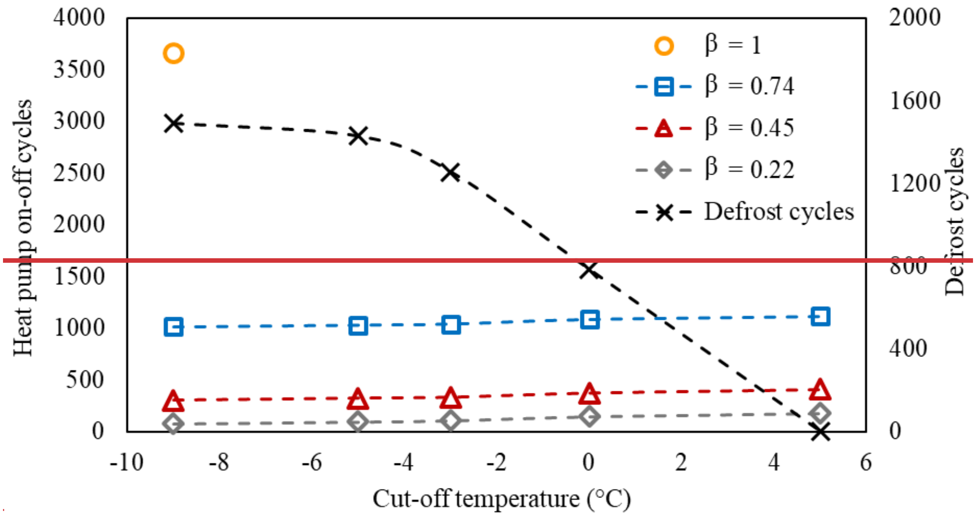
4000
3500
3000
2500
2000
1500
1000
500
0
2000
1600
1200
800
400
0
-10
-8
-6
-4
-2
0
2
4
6
Heat pump on-off cycles
Defrost cycles
Cut-off temperature (°C)
β = 1
β = 0.74
β = 0.45
β = 0.22
Defrost cycles

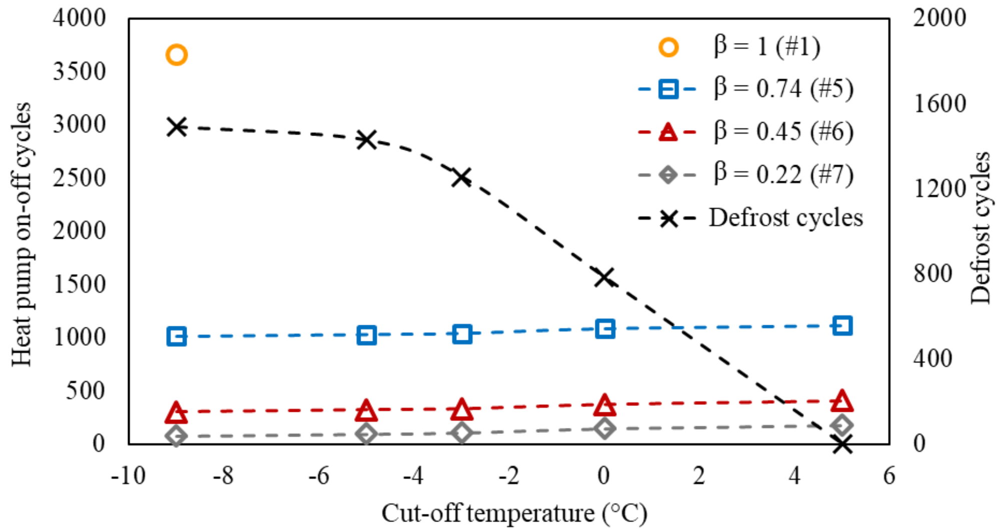
4000
3500
3000
2500
2000
1500
1000
500
0
2000
1600
1200
800
400
0
-10
-8
-6
-4
-2
0
2
4
6
Heat pump on-off cycles
Defrost cycles
Cut-off temperature (°C)
β = 1 (#1)
β = 0.74 (#5)
β = 0.45 (#6)
β = 0.22 (#7)
Defrost cycles

(a)

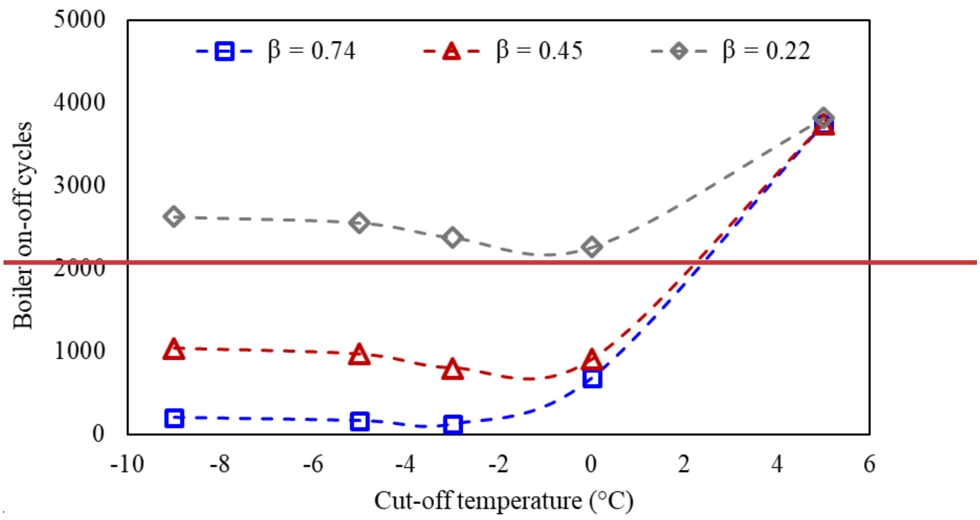

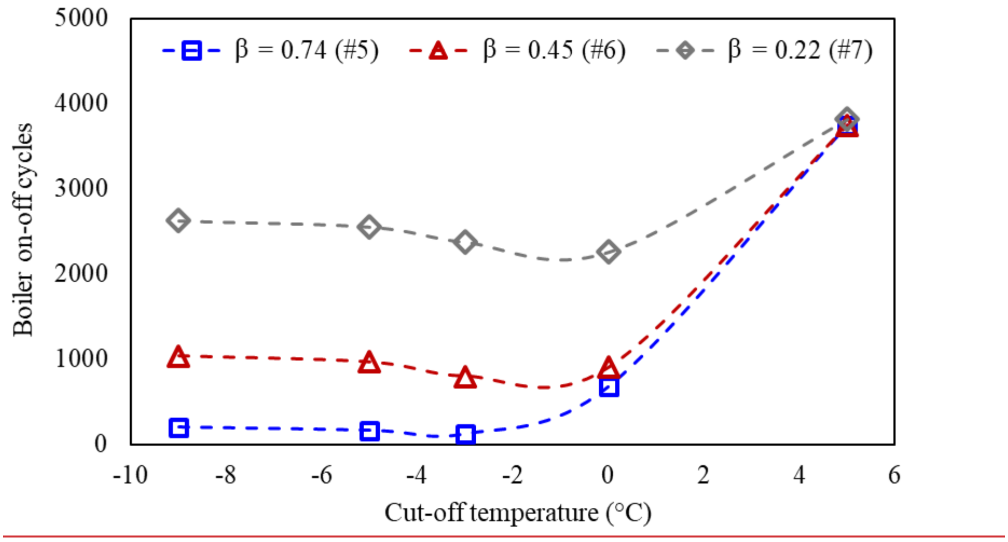

(b)

Figure 10. Seasonal number of defrost cycles, heat pump on-off cycles (a) and boiler on-off cycles (b) as functions of the peak load ratio and of the cut-off temperature

Moreover, the data depicted in Figure 10a highlight that the cut-off temperature has no significant influence on the cycling frequency of the heat pump: for a fixed value of the peak load ratio the number of on-off cycles performed by the heat pump during the heating season slightly raises when $T_{cut\text{-}off}$ increases. Furthermore, if compared to case #1 the number of on-off cycles diminishes up to 70%, 90% and 95% when the peak load ratio goes from 1 to 0.74, 0.45 and 0.22, respectively. However, this large reduction of performed cycles is not able to guarantee noticeable enhancement of the heat pump seasonal performance due to the low cycling energy losses of the selected units.

On the other hand, also the boiler seasonal efficiency is influenced by the number of on-off cycles carried out along the season, depicted in Figure 10b as a function of both the peak load ratio and the cut-off temperature. It is evident that the number of on-off cycles performed by the boiler raises when $T_{cut\text{-}off}$ increases and the heat pump size is reduced, according to a more frequent use of the back-up unit in place of the AWHP. For example, by fixing the cut-off temperature equal to -5°C, the number of cycles carried out by the boiler increases from 160 to 2551 when the peak load ratio decreases from 0.74 to 0.22; as a consequence, the boiler seasonal efficiency is reduced up to 7%.

Table 4. Influence of on-off cycles and defrost cycles on the seasonal energy efficiency of the system for cases #1 and #8

	Case #1				Case #8	
	With defrost and cycling losses	Without defrost losses	Without cycling losses	Without defrost and cycling losses	With cycling losses	Without cycling losses
η_S	1.05	1.13	1.06	1.14	0.91	1.01
Δ	-	+7.6%	+0.9%	+8.6%	-	+11%

In order to put in evidence the influence of the energy losses of both defrost and on-off cycles on the performance of the system, the seasonal energy performance (η_S) of monovalent configurations (i.e. case #1 and case #8) has been evaluated neglecting the penalization effect linked to on-off and defrost cycles. In Table 4 the system seasonal energy efficiency is reported for different conditions, by considering or neglecting the effect of on-off and defrost cycles for cases #1 and #8. The influence of the cycling losses on the seasonal performance factor of the heat pump (i.e. case #1) is negligible: according to the data shown in Table 4, the seasonal efficiency η_S decreases less than 1% due to on-off cycles. This result was expected since, as reported before, the considered heat pump is equipped with an EEV, which guarantees reduced penalization during on-off transients. On the contrary, defrost cycles energy losses have a significant impact on the heat pump seasonal efficiency: η_S varies from 1.13 of the ideal case, in which defrost cycles have not been considered, to 1.05, corresponding to a reduction larger than 7% on a seasonal basis. Of course, this result depends on the chosen location, which is characterized by a cold and humid winter in this case study, but this result highlights how the energy losses linked to defrosting cycles can be considered significant in ambient conditions typical of large part of Northern Italy, with an expected penalty on η_S ranging around 5-15%. This result underlines how, in order to evaluate in an accurate way the energy and economic feasibility of these hybrid systems, the energy losses linked to the defrosting cycles has to be always taken into account. Finally, it is evident that cycling losses play a significant role on the boiler seasonal performance: as reported in Table 4 for case #8, its seasonal efficiency decreases up to 10% due to on-off cycle energy penalties. In fact, as evidenced by Figure 8, during the winter season the boiler performs a higher number of cycles with respect to the heat pump (more than 8000 cycles along the season) and, additionally, it is characterized by larger energy losses for each cycle (see Table 1). For these reasons, on-off cycling losses cannot be neglected in dynamic simulations for hybrid systems in which a boiler is present.

In conclusion, HHP systems are able to guarantee slight primary energy savings if compared to conventional heating systems based on a single AWHP as heat generator (up to 6%), while a stronger reduction of the system primary energy consumption, up to 22%, can be obtained by hybrid configurations with respect to monovalent heating systems based on a gas boiler. The results of the simulations presented in this work highlight how the energy performance of this kind of systems can be improved if the heat pump size (thus, the peak load ratio) is optimized on the basis of the adopted back-up heater and, at the same time, if an optimal setting of the system control algorithm is done.

4. CONCLUSIONS

In this paper a numerical study on the energy performance during the heating season of hybrid heat pump (HHP) systems coupled to a reference residential building has been performed by means of a series of dynamic simulations made with TRNSYS. The hybrid systems investigated in this work are based on an air-to-water heat pump (AWHP), while an electric heater or a condensing gas boiler have been considered as back-up devices. These systems have been compared to traditional monovalent configurations (heat pump only or gas-fired boiler only) in order to assess the optimal ~~system~~ layout of the heating system which can guarantee the maximum primary energy savings.

~~The results presented in this paper confirm~~Hence, based on the obtained results, it is clear how the use of HHP systems could ensure significant primary energy savings if compared to conventional monovalent systems based on a single heat generator and these benefits strongly depend on the heat pump size, the back-up heater typology and the control strategy adopted for the activation of both the devices. The following statements concerning hybrid heat pump systems can be made:

- w~~W~~hen the cut-off temperature is set equal to the design temperature (i.e. pure parallel working mode), only a slight improvement of the system seasonal efficiency can be achieved with respect to traditional configurations, although a strong reduction of the heat pump on-off cycles is observed. In this case, the heat pump must be sized to satisfy at least 40% and 70% of the building design load, when a boiler or an electric heater are selected as back-up devices, respectively.
- ~~On the other hand,~~ when a gas-fired boiler is considered as back-up heater and for the alternative operating mode (i.e. when $T_{cut\text{-}off}$ is larger than T_{ext}), it is possible to define an optimal configuration of the system which maximizes its seasonal energy performance. For the site considered in these simulations and for each size of the heat pump, the maximum value of η_S is obtained when $T_{cut\text{-}off}$ is set equal to 0°C.
- ~~and~~ appreciable primary energy savings (up to 6% and to 22% with respect to the reference monovalent configurations based on an AWHP and a condensing gas boiler, respectively) can be achieved with a peak load ratio equal to 0.74 (which means that the heat pump is sized in order to cover up to 74% of the design thermal load).
- ~~Finally, results point out that~~ defrost cycles have a significant influence on the system seasonal energy efficiency (η_S), which is decreased between 5% and 15% in cold and humid climates, typical of Northern Italy, as the one considered in this paper.

- ~~On the other hand,~~ the effect of cycling losses is strictly correlated to the features of each heater: the results shown in this paper demonstrate how on-off cycles do not significantly affect the heat pump performance in presence of an EEV and a large inverter modulating range, while, on the contrary, cycling losses have a significant impact on the boiler seasonal efficiency especially for units with a limited modulating range.

REFERENCES

[1] R.A. Enker, G.M. Morrison, Analysis of the transition effects of building codes and regulations on the emergence of a low carbon residential building sector, Energy and Buildings 156 (2017) 40-50.

[2] European Union, Directive 2010/31/EU of the European Parliament and of the Council of 19 May 2010 on the Energy Performance of Buildings, European Union, Brussels, Belgium, 2010.

[3] European Union, Directive 2012/27/EU of the European Parliament and of the Council of 25 October 2012 on Energy Efficiency, amending Directives 2009/125/EC, European Union, Brussels, Belgium, 2012.

[4] European Union, Directive 2018/844 of the European Parliament and of the Council of 30 May 2018 amending Directive 2010/31/EU on the Energy Performance of Buildings and Directive 2012/27/EU on Energy Efficiency, Brussles, Belgium, 2018.

[5] European Commission, Communication from the Commission to the European Parliament, the Council, the European economic and social Committee and the Committee of the Regions – A policy framework for climate and energy in the period from 2020 to 2030, European Commission, Brussels, Belgium, 2014.

[6] ISTAT (Italian National Statistical Institute), Census 2011 of population and houses, 2011. Available from http://www.istat.it/it/censimento-popolazione/censimento-popolazione-2011.

[7] C. Treichel, C.A. Cruickshank, Greenhouse gas emissions analysis of heat pump water heaters coupled with air-based solar thermal collectors in Canada and the United States, Energy and Buildings 231 (2021) 110594.

[8] F. Knobloch, S.V. Hanssen, A. Lam, H. Pollitt, P. Salas, U. Chewpreecha, M.A.J. Huijbregts, J.F. Mercure, Net emission reductions from electric cars and heat pumps in 59 world regions over time, Nature Sustainability 3 (2020) 437-447.

[9] F. Madonna, F. Bazzocchi, Annual performances of reversible air-to-water heat pumps in small residential buildings, Energy and Buildings 65 (2013) 299-309.

[10] EHPA (European Heat Pump Association), European Heat Pump Market and Statistics Report 2015, 2016. Available from: http://www.ehpa.org/market-data/2015/.

[11] H. Wolisz, T. Schutz, T. Blanke, M. Hagenkamp, M. Kohrn, M. Wesseling, D. Muller, Cost optimal sizing of smart buildings' energy system components considering changing end-consumer electricity markets, Energy 137 (2017) 715-728.

[12] M. Qu, T. Li, S. Deng, Y. Fan, Z. Li, Improving defrosting performance of cascade air source heat pump using thermal energy storage based reverse cycle defrosting method, Applied Thermal Engineering 121 (2017) 728-736.

[13] J.Y. Jang, H.H. Bae, S.J. Lee, M.Y. Ha, Continous heating of an air-source heat pump during defrosting and improement of energy efficiency, Applied Energy 110 (2013) 9-16.

[14] Q. Minglu, X. Liang, S. Deng, J. Yiqiang, Improved indoor thermal comfort during defrost with a novel reverse-cycle defrosting method for air source heat pumps, Building and Environment 45 (2010) 2354-2361.

[15] G. Bagarella, R. Lazzarin, B. Lamanna, Cycling losses in refrigeration equipment: An experimental evaluation, International Journal of Refrigeration 36 (2013) 2111-2118.

[16] M. Pieve, R. Trinchieri, heat pump market report for Italy, Heat Pumping Technologies Magazine 36 (2018) 14-18.

[17] L. Bergmann, J. Jansen, The State of Play of the Hybrid Heat Pump Market, Delta Energy & Environment, 2015.

[18] H. Park, K.H. Nam, G.H. Jang, M.S. Kim, Performance investigation of heat pump-gas fired water heater hybrid system and its economic feasibility study, Energy and Buildings 80 (2014) 480-489.

[19] R. De Coninck, L. Helsen, Practical implementation and evaluation of model predictive control for an office building in Brussels, Energy and Buildings 111 (2016) 290-298.

[20] G. Li, Parallel loop configuration for hybrid heat pump – gas fired water heater system with smart control strategy, Appled Thermal Engineering 138 (2018) 807-818.

[21] G. Li, Y. Du, Performance investigation and economic benefits of new control-strategies for heat pump-gas fired water heater hybrid system, Applied Energy 232 (2018) 101-118.

[22] E. Zanetti, M. Aprile, D. Kum, R. Scoccia, M. Motta, Energy saving potentials of a photovoltaic assisted heat pump for hybrid building heating system via optimal control, Journal of Building Engineering 27 (2020) 100854.

[23] P. Fitzpastrick, F. D'Ettorre, M. De Rosa, M. Yadack, U. Eicker, D. P. Finn, Influence of electricity prices on energy flexibility of integrated hybrid heat pump and thermal storage systems in a residential building, Energy & Buildings 223 (2020) 110142.

[24] F. D'Ettorre, P. Conti, E. Schito, D. Testi, Model predictive control of a hybrid heat pump system and impact of the prediction horizon on cost-saving potential and optimal storage capacity, Applied Thermal Engineering 148 (2019) 524-535.

[25] T. S. Amirkhizi, I. G. Jensen. Cost comparison and optimization of gas electric hybrid heat pumps. WIREs Energy and Environment (2020) e370.

[26] Y. Ma, M. Zaheeruddin, Dynamic modeling, adaptive control and energy performance simulation of a hybrid hydronic space heating system, Building Services Engineering Research and Technology 39 (2018) 406-429.

[27] G. Bagarella, R. Lazzarin, M. Noro, Annual simulation, energy and economic analysis of hybrid heat pump systems for residential buildings, Applied Thermal Engineering 99 (2016) 485-494.

[28] D. Fischer, K.B. Lindberg, H. Madani, C. Wittwer, Impact of PV and variable prices on optimal system sizing for heat pumps and thermal storage, Energy and Buildings 128 (2016) 723-733.

[29] K. Klein, K. Huchtemann, D. Müller, Numerical study on hybrid heat pump systems in existing buildings, Energy and Buildings 69 (2014) 193-201.

[30] C. Di Perna, G. Magri, G. Giuliani, G. Serenelli, Experimental assessment and dynamic analysis of a hybrid generator composed of an air source heat pump coupled

with a condensing gas boiler in a residential building, Applied Thermal Engineering 76 (2015) 86-97.

[31] S.A. Klein et al., TRNSYS 17: A Transient System Simulation Program, Solar Energy Laboratory, University of Wisconsin, Madison, WI, USA, 2010.

[32] D.A. Waddicor, E. Fuentes, M. Azar, J. Salom, Partial load efficiency degradation of a water-to-water heat pump under fixed set-point control, Applied Thermal Engineering 106 (2016) 275-285.

[33] M. Dongellini, G.L. Morini, On-off cycling losses of reversible air-to-water heat pump systems as a function of the unit power modulation capacity, Energy Conversion and Management 196 (2019) 966-978.

[34] R. Dott, M. Haller, J. Ruschenburg, F. Ochs, J. Bony, IEA-SHC Task 44 Subtask C Technical Report: The Reference Framework for System Simulations of the IEA SHC Task 44 / HPP Annex 38: Part B: Buildings and Space Heat Load, IEA-SHC, 2013. (27th of October 2017).

[35] G. Bagarella, R. Lazzarin, M. Noro, Sizing strategy of on-off and modulating heat pump systems based on annual energy analysis, International Journal of Refrigeration 65 (2016) 183-193.

[36] Q. Minglu, X. Liang, D. Shiming, J. Yiqiang, A study of the reverse cycle defrosting performance on a multi-circuit outdoor coil unit in an air source heat pump – Part I: Experiments, Applied Energy 91 (2012) 122-129.

[37] P. Vocale, G.L. Morini, M. Spiga, Influence of outdoor air conditions on the air source heat pumps performance, Energy Procedia 45 (2014) 653-662.

[38] D. Huang, X. Yuan, X. Zhang, Effects of fan-starting methods on the reverse-cycle defrost performance of an air-to-water heat pump, International Journal of Refrigeration 27 (2004) 869-875.

[39] D. Huang, Q. Li, X. Yuan, Comparison between hot-gas bypass defrosting and reverse-cycle defrosting methods on an air-to-water heat pump, Applied Energy 86 (2009) 1697-1703.

[40] A.T. De La Cruz. P. Riviere, D. Marchio, O. Cauret, A. Milu, Hardware in the loop test bench using Modelica: A platform to test and improve the control of heating systems, Applied Energy 188 (2017) 107-120.

[41] Italian Republic, DPR 412/93, Regolamento recante norme per la progettazione, l'installazione, l'esercizio e la manutenzione degli impianti termici degli edifici ai fini del contenimento dei consumi di energia, 1993.

[42] TRNSYS 17 - A TRaNsient SYstem Simulation program, User Manual. Volume 5: Multizone Building Modeling with Type 56 and TRNBuild. Version 17.1, Solar Energy Laboratory, University of Wisconsin, Madison, USA, 2012.

[43] M.F. Fels, PRISM: An introduction, Energy and Buildings 9 (1986) 5-18.

[44] Decreto interministeriale 26 giugno 2015 - Applicazione delle metodologie di calcolo delle prestazioni energetiche e definizione delle prescrizioni e dei requisiti minimi degli edifici, 2015.

[45] CEN (European Committee for Standardization), Standard EN 14825:2016. Air Conditioners, Liquid Chilling Packages and Heat Pumps, with Electrically Driven Compressors, for Space Heating and Cooling – Testing and Rating at Part Load Conditions and Calculation of Seasonal Performance, 2016.